SECTION EDITOR: JANEY L. WIGGS, MD, PhD

ONLINE FIRST

Three-dimensional Distribution of the Vitelliform Lesion, Photoreceptors, and Retinal Pigment Epithelium in the Macula of Patients With Best Vitelliform Macular Dystrophy

Christine N. Kay, MD; Michael D. Abramoff, MD, PhD; Robert F. Mullins, PhD; Tyson R. Kinnick, PhD; Kyuongmoo Lee, PhD; Mari E. Eyestone, BS; Mina M. Chung, MD; Elliott H. Sohn, MD; Edwin M. Stone, MD, PhD

Objective: To describe the anatomical phenotypes of Best vitelliform macular dystrophy (BVMD) with spectral-domain optical coherence tomography (SD-OCT) in a large series of patients with confirmed mutations in the *BEST1* gene.

Methods: In our retrospective observational case series, we assessed 15 patients (30 eyes) with a clinical diagnosis of vitelliform macular dystrophy who were found to have mutations in the *BEST1* gene. Color fundus photographs and SD-OCT images were evaluated and compared with those of 15 age-matched controls (30 eyes). Using a validated 3-dimensional SD-OCT segmentation algorithm, we calculated the equivalent thickness of photoreceptors and the equivalent thickness of the retinal pigment epithelium for each patient. The photoreceptor equivalent thickness and the retinal pigment epithelium (RPE) equivalent thickness were compared in all patients, in a region of the macula outside the central lesion for patients with BVMD and outside the fovea in control patients. Paired *t* tests were used for statistical analysis.

Results: The SD-OCT findings revealed that the vitelliform lesion consists of material above the RPE and below the outer segment tips. Additionally, drusen-like deposition of sub-RPE material was notable, and several patients exhibited a sub-RPE fibrotic nodule. Patients with BVMD had a mean photoreceptor equivalent thickness of 28.3 μm, and control patients had a mean photoreceptor equivalent thickness of 21.8 μm, a mean difference of 6.5 μm ($P<.01$), whereas the mean RPE equivalent thickness was not statistically different between patients with BVMD and control patients ($P=.53$).

Conclusions: The SD-OCT findings suggest that vitelliform material is located in the subretinal space and that BVMD is associated with diffuse photoreceptor outer segment abnormalities overlying a structurally normal RPE.

Clinical Relevance: These findings provide new insight into the pathophysiology of BVMD and thus have implications for the development of therapeutic interventions.

Arch Ophthalmol. 2012;130(3):357-364.
Published online November 14, 2011.
doi:10.1001/archophthalmol.2011.363

Author Affiliations are listed at the end of this article.

BEST VITELLIFORM MACULAR dystrophy (BVMD) was originally described as an autosomal dominant form of macular degeneration that presents in childhood with a yellow yolk-like or vitelliform lesion in the macula.[1] Fishman and coworkers[2] found that 76% of patients younger than 40 years of age retain 20/40 visual acuity or better in at least 1 eye, whereas 74% of patients older than 30 years of age have visual acuity of 20/100 or worse in at least 1 eye. In addition to vision loss, patients with BVMD manifest a characteristic abnormal electrooculogram, with reduced light peak–to–dark trough ratios (Arden ratio, <1.5).[3] The light peak is mediated by changing chloride conductance across the basolateral plasma membrane of the retinal pigment epithelium (RPE).[4]

In 1992, Best disease was linked to 11q13 by studying a 5-generation family with 29 affected members,[5] and the localization was later refined to the pericentromeric region of chromosome 11.[6] The responsible gene, *VMD2* (now known as *BEST1*), was identified in 1998.[7,8] *BEST1* has 11 exons that span 14.1 kilobases and encodes a 585–amino acid protein. To date, nearly 200 disease-causing mutations have been identified in *BEST1*.[9-14] Several diseases have been linked to mutations in *BEST1*, including vitelliform macular dys-

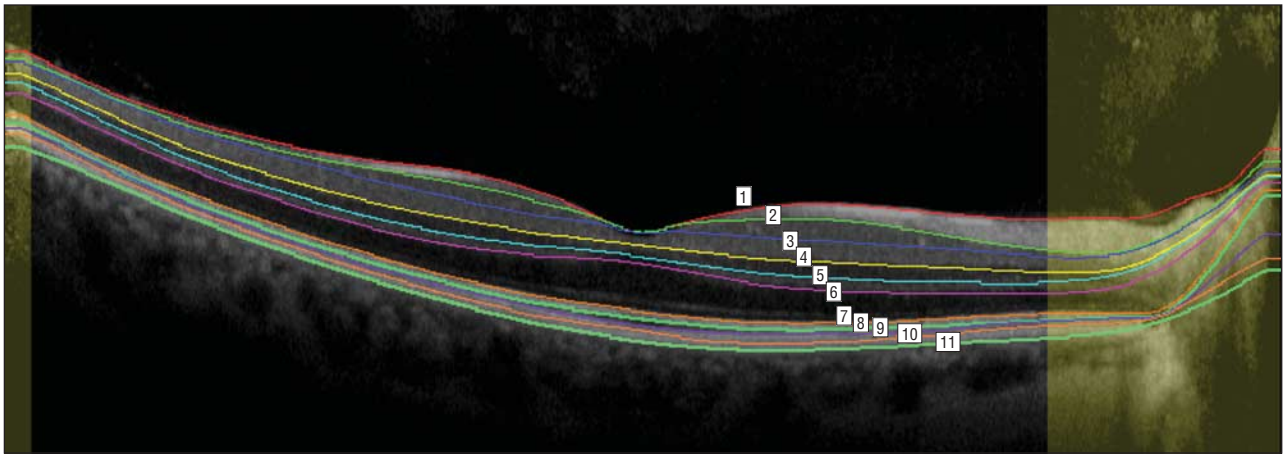

Figure 1. Depiction of 11 intraretinal surfaces: 1, internal limiting membrane; 2-3, ganglion cell layer; 3-4, inner plexiform layer; 4-5, inner nuclear layer; 5-6, outer plexiform layer; 6-7, outer nuclear layer; 7, external limiting membrane; 7-8, mitochondrial section of inner segments; 8, inner segment/outer segment junction; 9, outer segment tips; 10, inner surface of the retinal pigment epithelium (RPE); and 11, outer surface of RPE/Bruch's membrane. Using our 3-dimensional optical coherence tomographic (OCT) segmentation algorithm,[38] we were able to automatically determine these 11 intraretinal surfaces in all macular OCT scans.

trophy (both autosomal dominant and recessive), adult-onset foveal macular dystrophy, autosomal dominant vitreoretinochoroidopathy, and, most recently, retinitis pigmentosa.[15-21]

The localization of bestrophin-1 (BEST1), the protein encoded by *BEST1*, was determined to be in the basolateral plasma membrane of the RPE.[22] Physiological studies have provided evidence that human BEST1 functions as a Ca^{2+}-sensitive chloride channel[10,23-25] or plays a role in the regulation of Ca^{2+} channels.[26-29] Recently, a knock-in mouse model (W93C mutation in *BEST1*) revealed (1) enhanced accumulation of lipofuscin in the RPE and (2) debris that is thought to be unphagocytosed photoreceptor outer segments and lipofuscin granules in the subretinal space.[30]

The structural phenotype of the vitelliform lesion has been a subject of debate. Morphological findings described in BVMD donor eyes include (1) the abundant accumulation of lipofuscin in the RPE[31] (at least associated with some genotypes),[32] (2) the mislocalization of the BEST1 protein,[17,33] and (3) photoreceptor degeneration over a morphologically intact RPE layer.[33,34] None of the histopathologic analyses to date have sampled the vitelliform lesion because the patients who have been examined postmortem had largely progressed beyond this stage.

On the basis of histopathologic findings, researchers have suggested that BVMD affects a more diffuse region than that of the ophthalmoscopically visible lesion. Mullins et al[32] suggested that the predilection of the macula for Best disease–related lesions resulted from a relative paucity in normal eyes of wild-type bestrophin in macular locations compared with extramacular locations, suggesting that the entire macula might exhibit photoreceptor or RPE abnormalities rather than being limited to the central macula where lesions are clinically evident. Histopathologic findings from both Weingeist et al[31] and O'Gorman et al[35] suggested the accumulation of lipofuscin granules in the RPE with extrafoveal diffuse macular involvement.

The use of optical coherence tomography (OCT) makes it possible to anatomically examine the vitelliform lesion in vivo. For example, Querques et al[36] described the vitelliform lesion "at the level of the "RPE/photoreceptor complex," and Ferrara et al[37] described the vitelliform lesion as existing above the RPE and under the tips of the photoreceptor outer segments. Some of these OCT-guided studies were performed for patients with a clinical diagnosis of BVMD without molecular confirmation of disease. A more precise anatomic understanding of BVMD could provide insight into the pathophysiology of the disease and clinically relevant information for future therapeutic investigation, particularly with respect to the relative effect of the disease on photoreceptors as compared with the RPE. In our study, we investigate the 3-dimensional distribution of the vitelliform lesion and the anatomical condition of the RPE and photoreceptors in the maculas of patients with an array of *BEST1* mutations.

METHODS

Patients were retrospectively recruited on the basis of a clinical diagnosis of BVMD made by a board-certified ophthalmologist and on the basis of molecular confirmation of a mutation in the *BEST1* gene; the molecular testing was performed in our laboratory with bidirectional DNA sequencing using ABI 3730 sequencers (Applied Biosystems, Carlsbad, California). Normal controls were matched by age (within 5 years) to the patients with BVMD. These normal controls had normal outer retinas, as determined by a retinal specialist performing indirect ophthalmoscopy, and had no history of retinal disease, diabetes mellitus, or glaucoma.

All patients with BVMD and all control patients underwent OCT imaging using the Spectralis (Heidelberg, Germany) 3-dimensional volume, scan protocol ($6.0 \times 6.0 \times 2.2$ mm: 64 [y coordinate], 1048 [x coordinate], and 1024 [z coordinate] voxels, respectively). Color fundus photographs (Zeiss, Dublin, California) and visual acuities were obtained during the same visit. Using our validated, fully 3-dimensional OCT segmentation algorithm, we automatically determined 11 intraretinal surfaces, from the internal limiting membrane (layer 1) to Bruch's membrane (layer 11), in all macular OCT scans from both eyes for all patients (**Figure 1**).[38,39]

Using our OCT viewing software,[40] a retina specialist (C.K.) manually excluded a 3-dimensional region encompassing the

Table. Structural Features of Best Vitelliform Macular Dystrophy in 15 Patients

Patient Age, y	Mutation in *BEST1* Gene	Right Eye		Left Eye	
		Type of Lesion	Visual Acuity	Type of Lesion	Visual Acuity
17	Asp302Ala GAT>GCT	Pseudohypopyon	20/20	Fibrotic nodule	20/100
22	Asp302Ala GAT>GCT	Fibrotic nodule	20/50	Fibrotic nodule	20/20
22	Asp302Ala GAT>GCT	Fibrotic nodule	20/20	Fibrotic nodule	20/100
15	Tyr227Asn TAC>AAC	Vitelliform	20/40	Fibrotic nodule	20/30
84	Tyr227Asn TAC>AAC	Multifocal and vitelliform	20/40	Multifocal and vitelliform	20/60
54	Tyr227Asn TAC>AAC	Multifocal	20/15	Vitelliform	20/25
67	Asp301 del3gGAT	RPEDs and SRF	20/125	RPEDs and SRF	20/125
13	Arg218His CGT>CAT	Fibrotic nodule	20/70	Fibrotic nodule	20/25
68	Gln316Pro CAG>CCG	Vitelliform	20/30	No lesion	20/20
69	Glu300Lys GAG-AAG	RPEDs and SRF	20/30	RPEDs and SRF	20/20
54	Leu294 del3cTCA	Atrophic	20/125	Vitelliform	20/40
58	Lys30Arg ex 2	Subretinal fibrosis and SRF	20/50	Atrophic	20/70
30	Thr241Asn ACT>AAT	Fibrotic nodule	20/63	Pseudohypopyon	20/40
15	Thr307Ile ACC>ATC	Pseudohypopyon	20/20	Pseudohypopyon	20/20
42	Asn133Lys	Vitelliform	20/25 + 3	Atrophy and SRF	20/125

Abbreviations: RPEDs, retinal pigment epithelial detachments; SRF, subretinal fluid.

fovea and, if present, the central Best disease–related lesion from further analysis. Each age-matched case-control pair of patients was then evaluated. For each control patient, a region of exclusion was manually selected to match the volume of the region excluded in the corresponding age-matched patient with BVMD. Measurements of photoreceptor equivalent thickness over the entire macular scan region (excluding the fovea and lesion area as described) were automatically determined, for each A-scan, as the distance in micrometers between surface 8 (photoreceptor inner segment/outer segment junction) and surface 10 (inner surface of the RPE). Measurements of RPE equivalent thickness over the identical scan region were determined, for each A-scan, as the distance in micrometers between surface 10 (inner surface of the RPE) and surface 11 (outer surface of the RPE). The average photoreceptor equivalent thickness and the average RPE equivalent thickness were determined from these surface thicknesses. The mean photoreceptor equivalent thickness and the mean RPE equivalent thickness were calculated by averaging the photoreceptor equivalent thickness and the RPE equivalent thickness of each A-scan, for each eye and for each patient. The photoreceptor equivalent thickness differences and the RPE equivalent thickness differences between patients with BVMD and control patients were then statistically analyzed using a paired *t* test in Excel (Microsoft, Redmond, Washington) at a significance level of .05. Our study was approved by the institutional review board for human subjects research at the University of Iowa and adhered to the tenets set forth in the Declaration of Helsinki.

RESULTS

A total of 15 patients with BVMD (30 eyes) and 15 control patients (30 eyes) were included. There were a total of 11 mutations in the *BEST1* gene among the 15 patients with BVMD (**Table**). High-definition OCT findings revealed that the vitelliform lesion consists of material located in the subretinal space (**Figures 2** and **3**). Additionally, deposits of sub-RPE material were noted in the same space in which drusen accumulate, and several patients had a highly reflective dense nodule of material that was located under the RPE. This material is likely to be fibrotic scar tissue, given the similarity of this lesion to fibrovascular pigment epithelial detachments seen in age-related macular degeneration. There is an abrupt angle of the RPE contour due to the strong adherence of RPE cells to their basal lamina. Vitelliform lesions in the subretinal space are shown in Figures 2 and 3. In Figure 2, a vitelliform lesion seen during clinical examination is demonstrated to contain subretinal material on an OCT scan in a 68-year-old woman with a Gln316Pro mutation in *BEST1*. In this patient, the vitelliform lesion is localized to the subretinal space, with a gradual angle of departure of the reflectivity line that is typically seen with subretinal fluid accumulation. Another example of the subretinal location of the vitelliform lesion is demonstrated in a patient with a Tyr227Asn mutation in *BEST1* and 20/25 visual acuity (Figure 3). Atrophic lesions were characterized by disruption of the outer retina and the RPE. This feature is shown in **Figure 4**, which reveals atrophy of the RPE and loss of normal architecture of the overlying outer retina in a 58-year-old man with a Lys30Arg mutation in *BEST1*. In another case (ie, a 54-year-old man), multilayered vitelliform material was observed (**Figure 5**). This patient with a Tyr227Asn mutation in *BEST1* showed an extramacular lesion notable for material in multiple layers, including the sub–inner segment/outer segment junction, sub–outer segment tips, and sub-RPE space (Figure 5). In **Figure 6**, a sub-RPE fibrotic nodule is shown in a 31-year-old woman with a Thr241Asn mutation. The visual acuity in this eye was 20/63.

Automated measurements of photoreceptor equivalent thickness and RPE equivalent thickness could be performed for all patients. The mean photoreceptor equivalent thickness was 28.3 µm for patients with BVMD and 21.8 µm for control patients, an average difference of 6.5 µm (95% CI, –11.12 to –1.83 µm; $P < .01$). The mean RPE equivalent thickness was 24.5 µm for patients with BVMD and 25.1 µm for control patients, a nonsignificant dif-

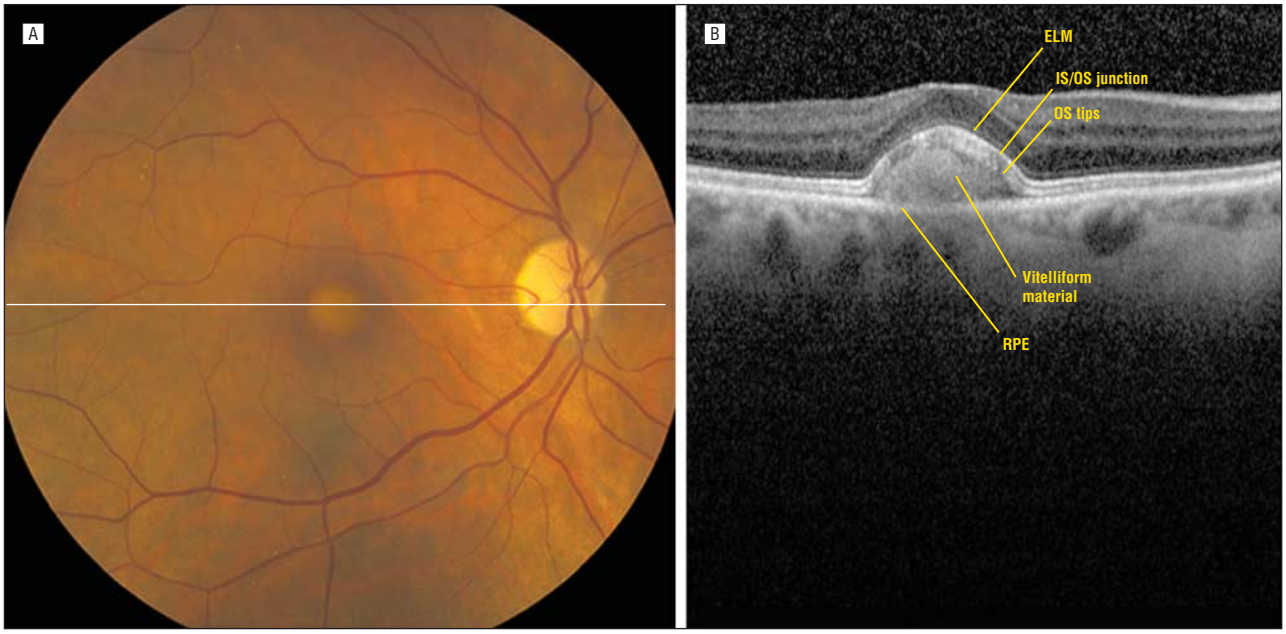

Figure 2. Classic vitelliform lesion (A) revealing subretinal vitelliform material (B) in a 68-year-old woman with a Gln316Pro Mutation in *BEST1*. The visual acuity of this eye was 20/30. ELM indicates external limiting membrane; IS/OS, inner segment/outer segment; RPE, retinal pigment epithelium.

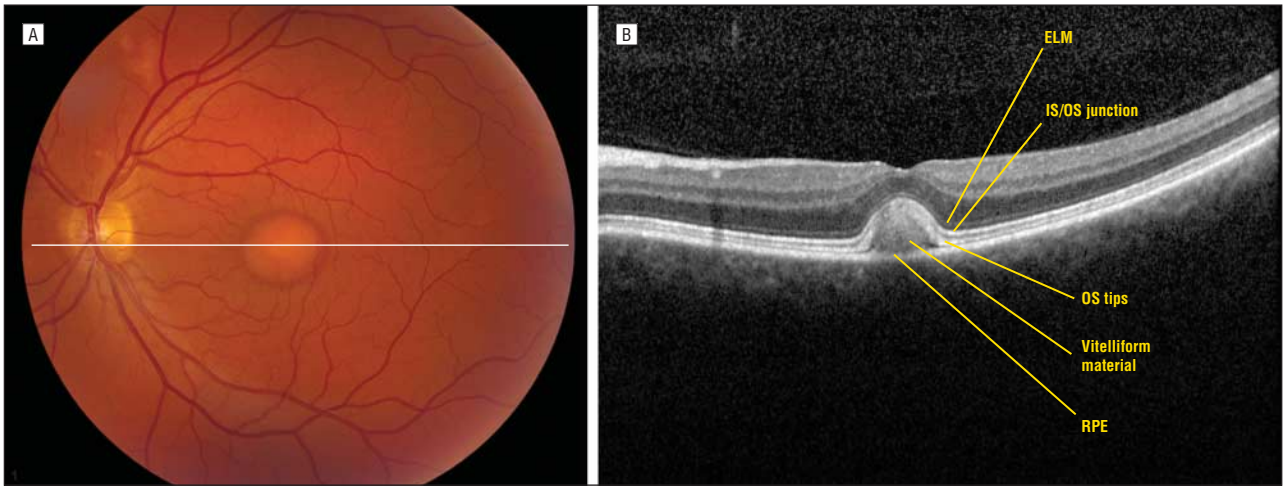

Figure 3. Classic vitelliform lesion (A) revealing subretinal vitelliform material (B) in a 54-year-old man with a Tyr227Asn mutation in *BEST1*. The visual acuity in this eye was 20/25. ELM indicates external limiting membrane; IS/OS, inner segment/outer segment; RPE, retinal pigment epithelium.

ference (95% CI, −1.19 to 2.21 µm; *P*=.53). The measurements of photoreceptor equivalent thickness and RPE equivalent thickness for each patient are shown in **Figures 7** and **8**.

We further sought to determine how genotype influenced the anatomical features of BVMD in the 15 patients with the disease. Only patients with the Tyr227Asn mutation (2 of the 3) showed extramacular flecks (compared with 0 of the 12 patients with other mutations). Fibrotic nodules were observed in 3 of the 3 patients (and 5 of the 6 eyes) with an Asp302Ala mutation. No other striking genotype-specific structural features were noted.

COMMENT

In our study, we used spectral-domain OCT to characterize the 3-dimensional anatomy of macular lesions in patients with confirmed mutations in the *BEST1* gene. The most common OCT-detected phenotypes that we observed were vitelliform material located in the subretinal space, fibrotic nodules under the RPE, and disruption and atrophy of the outer retina and the RPE. We also found that the retina adjacent to these ophthalmoscopically visible lesions was abnormal. Specifically, photoreceptor equivalent thickness was 6.5 µm thicker, on average, in patients with BVMD than in control patients, whereas, on average, the RPE of patients with BVMD was the same thickness as the RPE of control patients. This finding suggests that, although the abnormal protein encoded by *BEST1* is expressed in the RPE, its primary anatomical impact is at the photoreceptor level. These data are consistent with histopathologic findings of an attenuated outer retina overlying an intact RPE.[33] The photoreceptor equivalent thickness in patients with BVMD com-

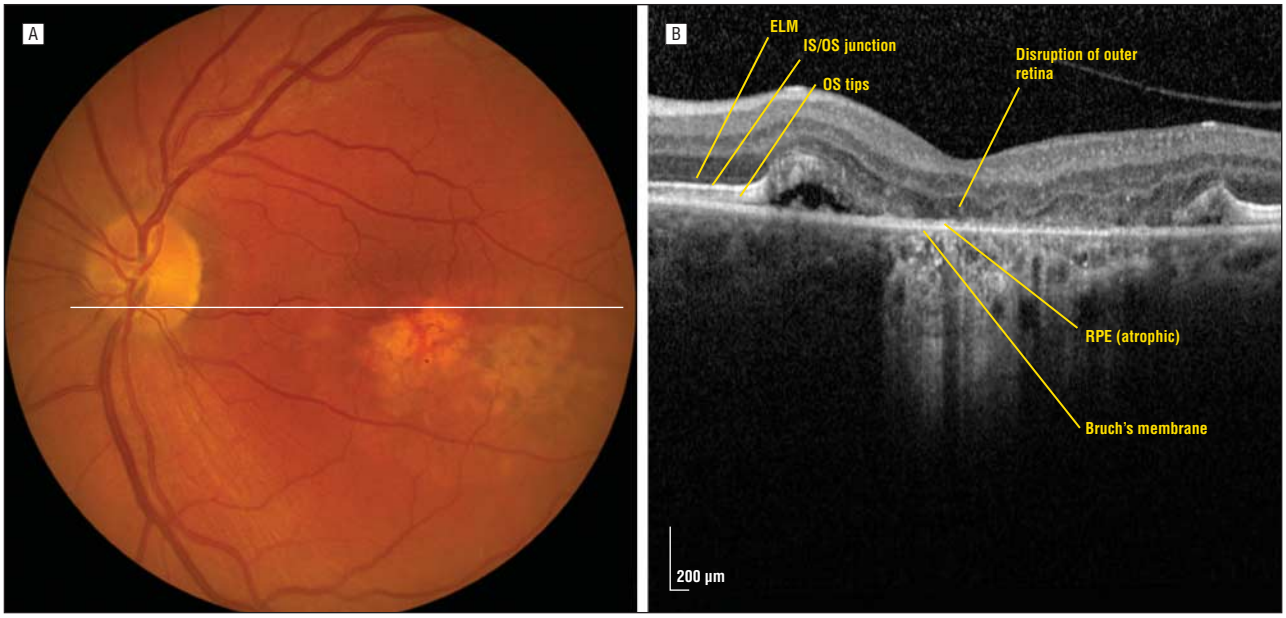

Figure 4. Atrophic lesion (A) revealing atrophy of the RPE and loss of normal architecture of the overlying outer retina (B) in a 58-year-old man with a Lys30Arg mutation in *BEST1*. The visual acuity in this eye was 20/70. ELM indicates external limiting membrane; IS/OS, inner segment/outer segment; RPE, retinal pigment epithelium.

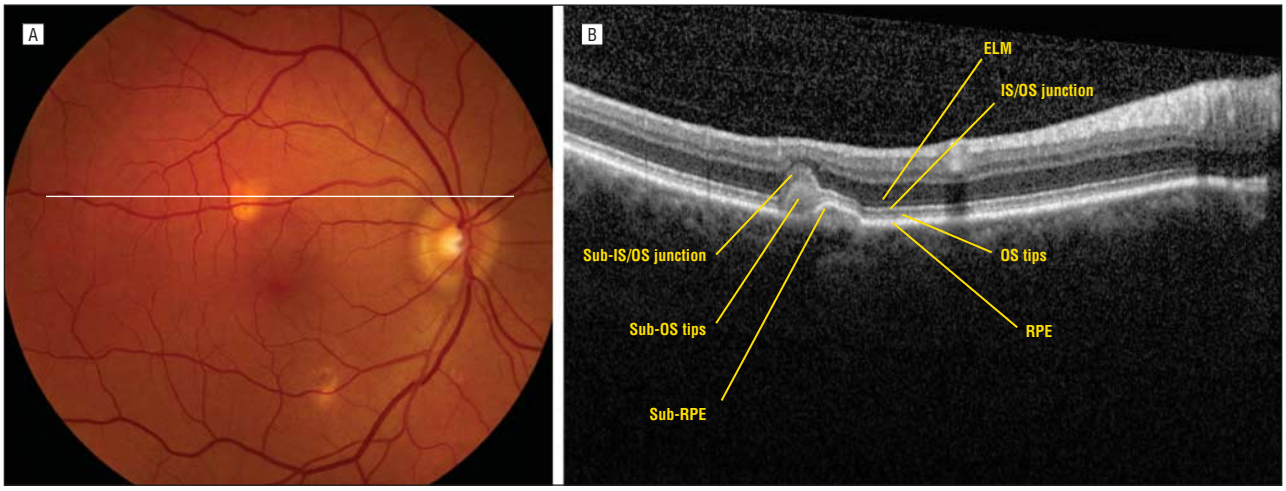

Figure 5. A, Extramacular lesion in a 54-year-old man with a Tyr227Asn mutation in *BEST1*. The visual acuity in this eye was 20/15. Material is notable in multiple layers (B), including the sub–inner segment/outer segment (sub-IS/OS) junction, the sub-OS tips, and beneath the retinal pigment epithelium (sub-RPE). ELM, indicates external limiting membrane.

pared with control patients increases with age, perhaps reflecting an age-related accumulation of outer segment debris as was seen in the histopathologic analysis of the knock-in mouse model.[30]

The diffuse photoreceptor involvement in BVMD that we found is consistent with the well-known abnormality of the electro-oculogram, a large-scale voltage-dependent phenomenon believed to originate from chloride conductance across the basolateral plasma membrane of the RPE. This phenomenon would be difficult to explain by a disease process limited to the macula.[4,41] Arden et al[41] found the electro-oculogram to be normal in patients with localized chorioretinal disease but abnormal when damage is diffuse and affects the majority of the choroid or the RPE. Lending further support to a model of diffuse involvement in BVMD is the immunohistochemical finding that bestrophin (at some level) is expressed to some degree in both the macular RPE and the peripheral RPE.[32]

Given prior physiological findings that bestrophin affects the function of the RPE by modulating ion channels, it is likely that the ionic milieu of the subretinal space is altered in BVMD. Our OCT analyses suggest that BVMD may be caused by RPE-mediated changes in the ionic environment of the subretinal space, leading to aberrant interaction between photoreceptors and the RPE, resulting in the accumulation of fluid and outer segment debris in the subretinal space. In normal individuals, the interphotoreceptor matrix is responsible for the tight adhesion of the photoreceptors to the RPE, and structural differences in this matrix have been reported in foveal and extrafoveal locations.[42] Such regional variations in this matrix may explain the macular location of the vitelliform lesion in

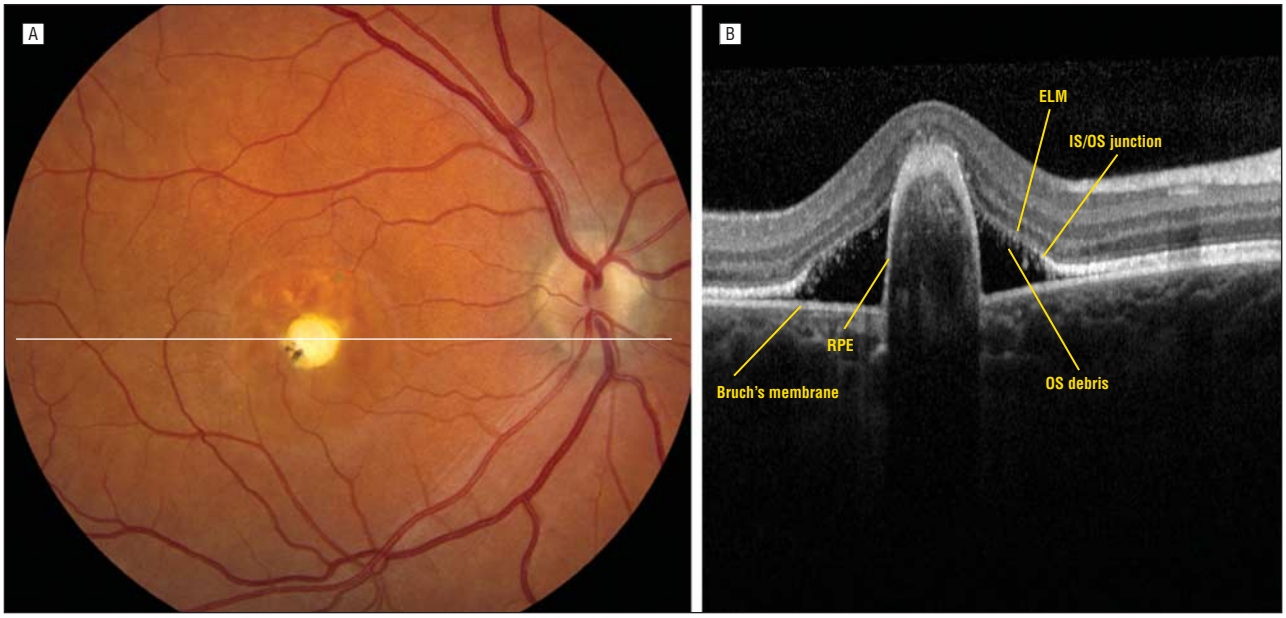

Figure 6. Subretinal pigment epithelium fibrotic nodule in a 31-year-old woman with a Thr241Asn mutation in *BEST1*. The visual acuity in this eye was 20/63. ELM indicates external limiting membrane; IS/OS, inner segment/outer segment; RPE, retinal pigment epithelium.

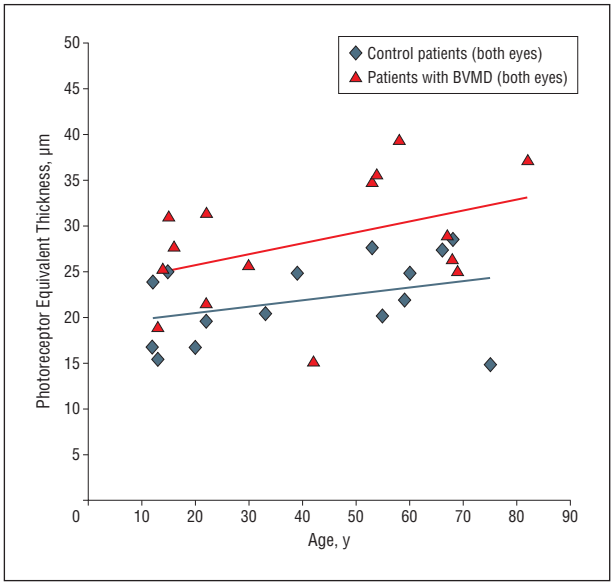

Figure 7. Measurements of photoreceptor equivalent thickness for each patient with Best vitelliform macular dystrophy (BVMD) and for each control patient. The mean photoreceptor equivalent thickness was 28.3 µm for patients with BVMD and 21.8 µm for age-matched control patients, an average difference of 6.5 µm (95% CI, −11.12 to −1.83 µm; $P<.01$).

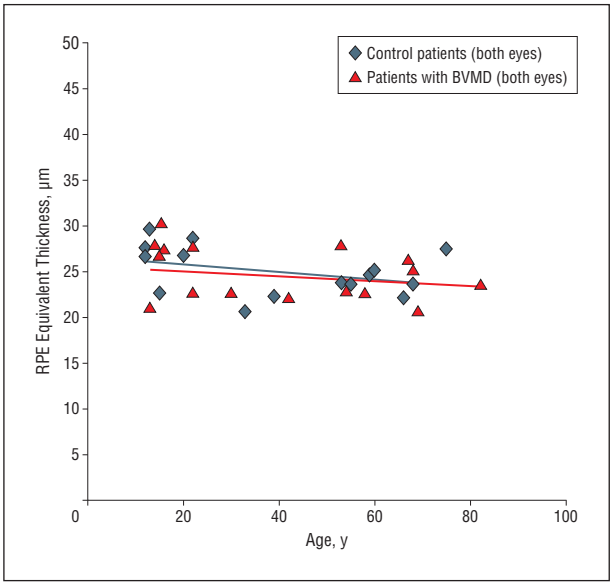

Figure 8. Measurements of retinal pigment epithelium (RPE) equivalent thickness for each patient with Best vitelliform macular dystrophy (BVMD) and for each control patient. The mean RPE equivalent thickness was 24.5 µm for patients with BVMD and 25.1 µm for control patients, a nonsignificant difference (95% CI, −1.19 to 2.21 µm; $P=.53$).

BVMD, despite diffuse photoreceptor involvement. Given the light-dependent nature of the electro-oculogram, it is also possible that altered bestrophin function affects other light-dependent events such as the circadian phagocytosis of outer segment tips. If so, the differences between the anatomy of the central macula and the anatomy of the more anterior retina could explain the location of the most characteristic BVMD-related lesion.[43]

Although it is not possible to draw conclusions regarding a phenotype-genotype correlation given the small numbers of patients with the same mutation, 2 suggestive trends were noted. Two of the 3 patients with a Tyr227Asn mutation had multifocal lesions compared with 0 of 12 patients with other genetic variants, and all 3 patients with the Asp302Ala GAT>GCT mutation revealed a fibrotic nodule at a young age, suggesting that the latter variant may be associated with a more severe fibrosis.

A notable limitation of our study is that it is not longitudinal, and although most patients have been followed for years, typically only 1 spectral-domain OCT image was available per eye. Future studies should include OCT analysis of photoreceptor equivalent thickness and RPE equivalent thickness in individual patients over time to document lesion progression.

In summary, we have provided additional evidence that the vitelliform material described in BVMD is located above the RPE and below the outer segment tips in the classic vitelliform lesion. We also showed that a sub-RPE phenotype exists that may best be described as a fibrotic scar. It is interesting to note that the photoreceptor cells overlying these fibrotic scars can survive for years and support good visual acuity (Table). Lastly, we found that the OCT correlate of photoreceptor outer segments (photoreceptor equivalent thickness) was, on average, 6.5 μm thicker among patients with BMVD than among control patients, whereas the OCT correlate of RPE thickness (RPE equivalent thickness) was not statistically different between patients with BVMD and control patients. Thus, although bestrophin is clearly expressed in the basolateral membrane of the RPE, the greatest anatomical effect of bestrophin dysfunction is a diffuse accumulation of material at the photoreceptor level.

Submitted for Publication: June 24, 2011; final revision received September 8, 2011; accepted September 22, 2011.
Published Online: November 14, 2011. doi:10.1001/archophthalmol.2011.363
Author Affiliations: Departments of Ophthalmology and Visual Sciences (Drs Kay, Abramoff, Mullins, Kinnick, Sohn, and Stone and Ms Eyestone), Electrical and Computer Engineering (Drs Abramoff and Lee), and Biomedical Engineering (Drs Abramoff and Lee), University of Iowa, Institute for Vision Research, University of Iowa Hospitals and Clinics (Drs Abramoff, Mullins, Kinnick, Chung, and Stone), and Department of Veterans Affairs, Center of Excellence for Prevention and Treatment of Visual Loss, and Veterans Affairs Medical Center (Dr Abramoff), Iowa City; Howard Hughes Medical Institute, Chevy Chase, Maryland (Dr Stone); and Flaum Eye Institute, University of Rochester, New York (Dr Chung).
Correspondence: Edwin M. Stone, MD, PhD, Department of Ophthalmology and Visual Sciences, University of Iowa Institute for Vision Research, 375 Newton Rd, 4111 MERF, Iowa City, IA 52242 (edwin-stone@uiowa.edu).
Financial Disclosure: Dr Abramoff has a patent application on some of the technology used in this study.
Funding/Support: This study was funded in part by the National Eye Institute (grant EY017451 to Dr Mullins, grant EY016822 to Dr Stone, and grants EY018853, EY019112, and EB004640 to Dr Abramoff), the Hansjoerg EJW Kolder Professorship in Best Disease Research (Dr Mullins), the Foundation Fighting Blindness, the Carver Endowment for Molecular Ophthalmology, the Carver Family Center for Macular Degeneration, the Howard Hughes Medical Institute (Dr Stone), Department of Veterans Affairs, and Research to Prevent Blindness.

REFERENCES

1. Best FZ. Über eine hereditäre Maculaaffektion. *Z Augenheilkunde*. 1905;13:199-212. doi:10.1159/000290318.
2. Fishman GA, Baca W, Alexander KR, Derlacki DJ, Glenn AM, Viana M. Visual acuity in patients with Best vitelliform macular dystrophy. *Ophthalmology*. 1993;100(11):1665-1670.
3. Krill AE, Morse PA, Potts AM, Klien BA. Hereditary vitelliruptive macular degeneration. *Am J Ophthalmol*. 1966;61(6):1405-1415.
4. Gallemore RP, Steinberg RH. Effects of DIDS on the chick retinal pigment epithelium: II, mechanism of the light peak and other responses originating at the basal membrane. *J Neurosci*. 1989;9(6):1977-1984.
5. Stone EM, Nichols BE, Streb LM, Kimura AE, Sheffield VC. Genetic linkage of vitelliform macular degeneration (Best's disease) to chromosome 11q13. *Nat Genet*. 1992;1(4):246-250.
6. Weber BH, Vogt G, Stöhr H, Sander S, Walker D, Jones C. High-resolution meiotic and physical mapping of the Best vitelliform macular dystrophy (VMD2) locus to pericentromeric chromosome 11. *Am J Hum Genet*. 1994;55(6):1182-1187.
7. Petrukhin K, Koisti MJ, Bakall B, et al. Identification of the gene responsible for Best macular dystrophy. *Nat Genet*. 1998;19(3):241-247.
8. Marquardt A, Stöhr H, Passmore LA, Krämer F, Rivera A, Weber BH. Mutations in a novel gene, VMD2, encoding a protein of unknown properties cause juvenile-onset vitelliform macular dystrophy (Best's disease). *Hum Mol Genet*. 1998;7(9):1517-1525.
9. Sun H, Tsunenari T, Yau KW, Nathans J. The vitelliform macular dystrophy protein defines a new family of chloride channels. *Proc Natl Acad Sci U S A*. 2002;99(6):4008-4013.
10. Tsunenari T, Sun H, Williams J, et al. Structure-function analysis of the bestrophin family of anion channels. *J Biol Chem*. 2003;278(42):41114-41125.
11. Bakall B, Marknell T, Ingvast S, et al. The mutation spectrum of the bestrophin protein—functional implications. *Hum Genet*. 1999;104(5):383-389.
12. Krämer F, White K, Pauleikhoff D, et al. Mutations in the VMD2 gene are associated with juvenile-onset vitelliform macular dystrophy (Best disease) and adult vitelliform macular dystrophy but not age-related macular degeneration. *Eur J Hum Genet*. 2000;8(4):286-292.
13. Sohn EH, Francis PJ, Duncan JL, et al. Phenotypic variability due to a novel Glu292Lys variation in exon 8 of the BEST1 gene causing Best macular dystrophy. *Arch Ophthalmol*. 2009;127(7):913-920.
14. Kinnick TR, Mullins RF, Dev S, et al. Autosomal recessive vitelliform macular dystrophy in a large cohort of vitelliform macular dystrophy patients. *Retina*. 2011;31(3):581-595.
15. Kaufman SJ, Goldberg MF, Orth DH, Fishman GA, Tessler H, Mizuno K. Autosomal dominant vitreoretinochoroidopathy. *Arch Ophthalmol*. 1982;100(2):272-278.
16. Lotery AJ, Munier FL, Fishman GA, et al. Allelic variation in the VMD2 gene in Best disease and age-related macular degeneration. *Invest Ophthalmol Vis Sci*. 2000;41(6):1291-1296.
17. Bakall B, Radu RA, Stanton JB, et al. Enhanced accumulation of A2E in individuals homozygous or heterozygous for mutations in BEST1 (VMD2). *Exp Eye Res*. 2007;85(1):34-43.
18. Gass JD. A clinicopathologic study of a peculiar foveomacular dystrophy. *Trans Am Ophthalmol Soc*. 1974;72:139-156.
19. Patrinely JR, Lewis RA, Font RL. Foveomacular vitelliform dystrophy, adult type: a clinicopathologic study including electron microscopic observations. *Ophthalmology*. 1985;92(12):1712-1718.
20. Davidson AE, Millar ID, Urquhart JE, et al. Missense mutations in a retinal pigment epithelium protein, bestrophin-1, cause retinitis pigmentosa. *Am J Hum Genet*. 2009;85(5):581-592.
21. Burgess R, Millar ID, Leroy BP, et al. Biallelic mutation of BEST1 causes a distinct retinopathy in humans. *Am J Hum Genet*. 2008;82(1):19-31.
22. Marmorstein AD, Marmorstein LY, Rayborn M, Wang X, Hollyfield JG, Petrukhin K. Bestrophin, the product of the Best vitelliform macular dystrophy gene (VMD2), localizes to the basolateral plasma membrane of the retinal pigment epithelium. *Proc Natl Acad Sci U S A*. 2000;97(23):12758-12763.
23. Hartzell HC, Qu Z, Yu K, Xiao Q, Chien LT. Molecular physiology of bestrophins: multifunctional membrane proteins linked to Best disease and other retinopathies. *Physiol Rev*. 2008;88(2):639-672.
24. Hartzell C, Qu Z, Putzier I, Artinian L, Chien LT, Cui Y. Looking chloride channels straight in the eye: bestrophins, lipofuscinosis, and retinal degeneration. *Physiology (Bethesda)*. 2005;20:292-302.
25. Xiao Q, Prussia A, Yu K, Cui YY, Hartzell HC. Regulation of bestrophin Cl channels by calcium: role of the C terminus. *J Gen Physiol*. 2008;132(6):681-692.
26. Rosenthal R, Bakall B, Kinnick T, et al. Expression of bestrophin-1, the product of the VMD2 gene, modulates voltage-dependent Ca2+ channels in retinal pigment epithelial cells. *FASEB J*. 2006;20(1):178-180.
27. Marmorstein LY, Wu J, McLaughlin P, et al. The light peak of the electroretinogram is dependent on voltage-gated calcium channels and antagonized by bestrophin (best-1). *J Gen Physiol*. 2006;127(5):577-589.
28. Marmorstein AD, Kinnick TR. Focus on molecules: bestrophin (best-1). *Exp Eye Res*. 2007;85(4):423-424.
29. Yu K, Xiao Q, Cui G, Lee A, Hartzell HC. The Best disease-linked Cl-channel hBest1 regulates Ca V 1 (L-type) Ca2+ channels via src-homology-binding domains. *J Neurosci*. 2008;28(22):5660-5670.
30. Zhang Y, Stanton JB, Wu J, et al. Suppression of Ca2+ signaling in a mouse model of Best disease. *Hum Mol Genet*. 2010;19(6):1108-1118.
31. Weingeist TA, Kobrin JL, Watzke RC. Histopathology of Best's macular dystrophy. *Arch Ophthalmol*. 1982;100(7):1108-1114.
32. Mullins RF, Kuehn MH, Faidley EA, Syed NA, Stone EM. Differential macular and

peripheral expression of bestrophin in human eyes and its implication for Best disease. *Invest Ophthalmol Vis Sci*. 2007;48(7):3372-3380.
33. Mullins RF, Oh KT, Heffron E, Hageman GS, Stone EM. Late development of vitelliform lesions and flecks in a patient with Best disease: clinicopathologic correlation. *Arch Ophthalmol*. 2005;123(11):1588-1594.
34. Frangieh GT, Green WR, Fine SL. A histopathologic study of Best's macular dystrophy. *Arch Ophthalmol*. 1982;100(7):1115-1121.
35. O'Gorman S, Flaherty WA, Fishman GA, Berson EL. *Arch Ophthalmol*. 1988;106 (9):1261-1268.
36. Querques G, Regenbogen M, Quijano C, Delphin N, Soubrane G, Souied EH. High-definition optical coherence tomography features in vitelliform macular dystrophy. *Am J Ophthalmol*. 2008;146(4):501-507.
37. Ferrara DC, Costa RA, Tsang S, Calucci D, Jorge R, Freund KB. Multimodal fundus imaging in Best vitelliform macular dystrophy. *Graefes Arch Clin Exp Ophthalmol*. 2010;248(10):1377-1386.
38. Haeker M, Sonka M, Kardon R, Shah V, Wu X, Abràmoff M. Automated segmentation of intraretinal layers from macular optical coherence tomography images. In: Pluim JPW, Reinhardt JM, eds. *Medical Imaging 2007: Image Processing (Proceedings of SPIE Vol. 6512)*. Bellingham, WA: SPIE Press; 2007:651214.
39. Garvin MK, Abràmoff MD, Wu X, Russell SR, Burns TL, Sonka M. Automated 3-D intraretinal layer segmentation of macular spectral-domain optical coherence tomography images. *IEEE Trans Med Imaging*. 2009;28(9):1436-1447.
40. van Dijk HW, Verbraak FD, Stehouwer M, et al. Association of visual function and ganglion cell layer thickness in patients with diabetes mellitus type 1 and no or minimal diabetic retinopathy. *Vision Res*. 2011;51(2):224-228.
41. Arden GB, Barrada A, Kelsey JH. New clinical test of retinal function based upon the standing potential of the eye. *Br J Ophthalmol*. 1962;46(8):449-467.
42. Hollyfield JG, Varner HH, Rayborn ME. Regional variation within the interphotoreceptor matrix from fovea to the retinal periphery. *Eye (Lond)*. 1990;4(pt 2): 333-339.
43. Anderson DH, Fisher SK. The relationship of primate foveal cones to the pigment epithelium. *J Ultrastruct Res*. 1979;67(1):23-32.

OBITUARY

In Memoriam: Mitchell H. Friedlaender, MD (1946-2011)

The first time I met Mitchell Friedlaender was in 1988 when I was interviewing at Scripps Clinic. He was the junior ophthalmologist in the department at the time. He had joined 3 years earlier. After those first few minutes with him, I walked out of his office with a terrific first impression of Scripps. He was helpful, encouraging, and supportive from the start. He continued to be so during his many years of service at Scripps Clinic.

Over the course of his career, his influence benefited both his close colleagues and the field of ophthalmology at large. At the clinical level, he was a stabilizing presence and brought marvelous interpersonal skills and goodwill to our daily work. Most people he came in contact with considered him a friend. He cared deeply for his patients, many of whom stayed with him in excess of 25 years. He also contributed vastly to our knowledge of ocular allergy and dry eye through his extensively published research and the hundreds of lectures he gave in the United States and abroad. With little fanfare, he founded and perpetuated valuable forums for information exchange, such as the Aspen Corneal Society in Snowmass, Colorado, and the Pearls of Ocular Therapy in La Jolla, California.

Mitch was a devoted family man. His busy office seemed to get smaller and smaller over the years as pictures of his wife and 2 children shared space with his many diplomas and awards. He pursued personal interests with equal enthusiasm, as he mastered the piano and the Japanese language and avidly collected Chicano art.

With characteristic devotion, Mitch was working up until a few days before his passing. I visited with him in his office at that time, not knowing it was the last time I would see him. He was, as always, kindly and positive. I realized, leaving his office that evening, that nothing had changed.

Mitchell Friedlaender will be sorely missed by his colleagues, along with his family. His life and his career ended too soon. The consolation for me and the rest of us who practice ophthalmology is that the work we do as we go forward will continue to be enhanced by Mitch's many valuable contributions.

K. Victor Zablit, MD

Author Affiliation: Division of Ophthalmology, Scripps Clinic, La Jolla, California.
Correspondence: Dr Zablit, Division of Ophthalmology, Scripps Clinic, La Jolla, CA 92037 (zablit.victor@scrippshealth.org).
Financial Disclosure: None reported.